

SU-8 serial MEMS switch for flexible RF applications

This content has been downloaded from IOPscience. Please scroll down to see the full text.

2011 J. Micromech. Microeng. 21 025010

(<http://iopscience.iop.org/0960-1317/21/2/025010>)

View [the table of contents for this issue](#), or go to the [journal homepage](#) for more

Download details:

IP Address: 140.113.38.11

This content was downloaded on 25/04/2014 at 00:55

Please note that [terms and conditions apply](#).

SU-8 serial MEMS switch for flexible RF applications

Tzu-Yuan Chao, M C Hsu, C-D Lin and Y T Cheng

Microsystems Integration Laboratory, Department of Electronics Engineering, National Chiao Tung University, 1001 Ta Hsueh Road, Hsinchu 30010, Taiwan

E-mail: buck34.ce92g@nctu.edu.tw, ytcheng@mail.nctu.edu.tw

Received 23 September 2010, in final form 30 November 2010

Published 11 January 2011

Online at stacks.iop.org/JMM/21/025010

Abstract

This paper presents a novel SU-8 micromachining process for MEMS series switch fabrication. The switch is designed with a clamped-clamped SU-8 ($5\ \mu\text{m}$)/Cu ($2\ \mu\text{m}$)/SU-8 ($3\ \mu\text{m}$) beam structure driven by electrostatic force, which is fabricated on a silicon substrate with a resistivity of $\sim 5\ \Omega\ \text{cm}$. Experimental results show that the switch can exhibit better than $-4.48\ \text{dB}$ insertion loss and $-28.2\ \text{dB}$ isolation up to 12 GHz. Such a large insertion loss is mainly caused by substrate loss which can be further reduced down to $-0.75\ \text{dB}$ as long as the substrate resistivity is increased up to $100\ \Omega\ \text{cm}$.

1. Introduction

Flexible electronics have attracted a lot of research attention in recent years due to their various potential applications such as flexible displays, stretchable solar cells, wearable wireless sensors and circuit systems. One of the technical challenges in the development of flexible electronics is fabrication temperature limitation due to the low glass transition point of a substrate. The flexible electronics fabricated on an organic substrate are generally accompanied by the characteristics of light weight, high flexibility, and low manufacture cost. However, the temperature limitation ($<200\ ^\circ\text{C}$) makes existing semiconductor processing techniques impracticable for the device fabrication of flexible electronics that require new materials with low manufacturing temperature characteristics [1–6].

Previously, Chang *et al* developed a customized low-temperature high-density inductively coupled plasma chemical vapor deposition (HDICPCVD) technique to deposit SiN_x at $100\ ^\circ\text{C}$ for the fabrication of RF MEMS on a printed circuit board [1]. Guo *et al* utilized a special glue to thermally compressive bonded thin Si wafer (50–100 nm thick) with a flexible FR-4 substrate (0.1 mm thick) so that the Si-based active MOS transistors and RF passive components can be transferred onto the flexible substrate with superior device performance [2]. In addition, Yuan *et al* proposed a silicon on insulator (SOI) wafer transferring technique whose processing temperature can be controlled well below $120\ ^\circ\text{C}$ to demonstrate single-crystal Si thin-film transistors on a

flexible polymer with the unit gain cut-off frequency, f_T , of 1.9 GHz and the maximum oscillation frequency, f_{max} , of 3.1 GHz [3]. Thus, in the paper, a new low-temperature SU-8 micromachining process is developed for RF MEMS passive fabrication. Unlike the aforementioned techniques which require special tools or might have low manufacturing yield during wafer transferring, such a low-temperature fabrication scheme only combining with spin coating and electroplating techniques can provide an alternative to realize cost-effective RF MEMS for flexible RF applications.

SU-8, a photo-definable plastic polymer invented by IBM, has been widely used for MEMS fabrication in recent years due to several superior material properties including excellent chemical stability for good biocompatibility, transparency to visible light suitable for device fabrication with a high aspect ratio, and low Young's modulus ($\sim 3.4\ \text{GPa}$) for better structure flexibility. Besides, its low processing temperature characteristic makes it a fascinating material for RF MEMS fabrication on a flexible substrate. On the other hand, RF MEMS switches possess a lot of advantages such as low series resistance, high isolation, and inherently negligible inter-modulation distortion [7]. It, therefore, has become a key component in the next generation radio-frequency integrated circuit (RFIC) systems. Previously, Shi *et al* had already demonstrated the first SU-8 MEMS switch with a lateral, direct contact beam structure for potential RF applications [8]. Although the switch with a self-cleaning design exhibits not only a low contact resistance but also a longer device lifetime, the lateral contact structure still needs further design

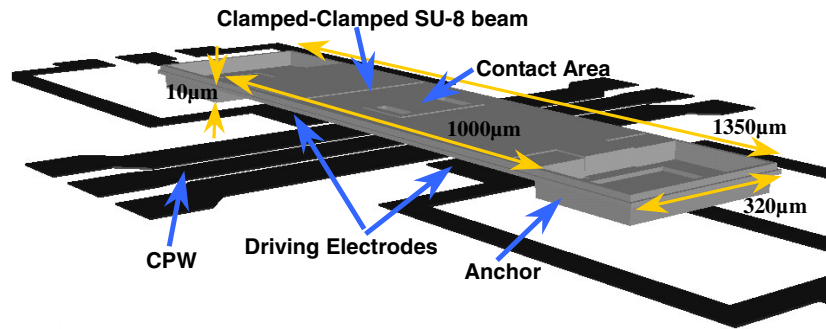


Figure 1. The scheme of the clamped–clamped SU-8 beam MEMS series switch.

to be integrated with conventional transmission lines for RFIC application that requires the design of 50Ω characteristic impedance and mode-matched transition. Thus, this paper will present a typical RF MEMS series switch fabricated using the proposed low-temperature SU-8 micromachining technique to demonstrate the process feasibility for the application of flexible electronics.

2. Fabrication process

The switch is designed with an electrostatically actuated clamped–clamped beam structure as shown in figure 1, which is a conventional MEMS series switch. The switch is fabricated on the top of a 50Ω coplanar waveguide (CPW). There is a $100 \mu\text{m}$ separation between two disconnected $450 \mu\text{m}$ long, $76 \mu\text{m}$ wide signal lines which would be connected if the switch is operated at ‘on’ state. The clamped–clamped beam structure of the switch is $1350 \mu\text{m}$ long, $320 \mu\text{m}$ wide and has a $10 \mu\text{m}$ gap spacing between the upper and lower driving electrodes. The beam is made of an SU-8/Cu/SU-8 sandwich layer to effectively eliminate the effect of induced residual stress on device performance. According to the switch design of Hyman *et al* [9], a sandwich layer structure could ease the coefficient of thermal expansion (CTE) mismatch that causes structural bending due to process temperature variance. After the beam is released, the stress compensation in the sandwich layer can further enhance device reliability.

Figure 2 shows the schematic process flow of the proposed SU-8 MEMS switch. The fabrication starts with $0.7 \mu\text{m}$ thick wet thermal oxidation at 1050°C for 2 h for electrical isolation on a commercial $4''$ silicon wafer with a resistivity of around $5 \Omega \text{cm}$ as shown in figure 2(a). As shown in figure 2(b), a layer of Ti (100 \AA)/Cu (1200 \AA) is then dc sputter-deposited as a seed layer covered by $7 \mu\text{m}$ thick AZ4620 which is two-step spin-coated at 1000 rpm for 15 s and 3500 rpm for 25 s, soft baked at 90°C for 5 min, exposed at a dose of 180 mJ cm^{-2} , developed using a dilute AZ400K developer (1:4 AZ400K:DI water), and selectively electroplated with $1.2 \mu\text{m}$ thick Cu with a current density of about 1 A dm^{-2} for 270 s as the aforementioned structure fabrication of the CPW, the ground plane, and the bottom biasing electrodes that are used for beam actuation. After removing AZ4620 and the Ti/Cu seed layer using acetone, buffered oxide etch (BOE) and CR-7T, a $10 \mu\text{m}$ thick negative photoresist (PR),

JSR THB-120N [10], is spin-coated at 2500 rpm for 40 s, soft baked at 100°C for 11 min, exposed at a dose of 1200 mJ cm^{-2} , patterned using 5% TMAH as a developer, and then hard baked at 120°C for 15 min as a sacrificial layer for the suspended switch structure fabrication as shown in figure 2(c). The thickness of JSR will define the initial gap between the contact metal of the switch and the CPW signal line underneath the contact. The gap spacing determines the switch isolation while it is operated at ‘off’ state. Once the JSR layer is defined, the first $3 \mu\text{m}$ thick SU-8 (GM1040) layer is spin-coated at 1100 rpm for 40 s, soft baked at 95°C for 15 min, exposed at a dose 400 mJ cm^{-2} , developed by an SU-8 developer (PGMEA), and then hard baked at 135°C for 60 min as the beam structure of the switch. However, due to the non-uniformity resulting from spin-coating on the $10 \mu\text{m}$ thick sacrificial layer, the thickness of the first SU-8 layer is measured to be about $5 \mu\text{m}$ by the surface profiler ET-4000 (Kosaka Laboratory Ltd). Prior to the hard baking, the SU-8 must be photo-patterned for the mechanical anchor and electrical contact fabrication of the switch. The anchor and metal contact are used for connecting the metal layer of the switch beam to the electrode for biasing the switch structure and to the CPW for electrical contact, respectively. Thus, before depositing a secondary Cu layer, the unmasked JSR region is slightly etched with the O_2 plasma reactive ion etching (RIE) process to expose a part of the metal layer deposited later for the switch contact as shown in figure 2(d).

For the secondary Cu layer deposition of the switch, another layer of Ti (100 \AA)/Cu (1200 \AA) is dc sputtered as the seed layer covered by $7 \mu\text{m}$ patterned AZ4620 PR for $2 \mu\text{m}$ thick selective Cu electroplating (1 A dm^{-2} , 330 s) as shown in figure 2(e). After electroplating Cu, the patterned AZ 4620 and Ti/Cu are stripped first and then another layer of $3 \mu\text{m}$ thick SU-8 is spin-coated, photo-patterned under the same condition as described above, and hard baked at 135°C for 60 min again as shown in figure 2(f). Finally, the JSR sacrificial layer is removed using JSR stripper THB-S1 at room temperature until the sacrificial layer is totally removed to form a freely suspended MEMS series switch as shown in figure 2(g). The as-fabricated switch structure contains two layers of SU-8 and one Cu layer within. Figure 3 shows optical micrographs taken from one end of the switch before and after stripping away the JSR sacrificial layer. It is clearly shown that the removal of the JSR layer can be observed

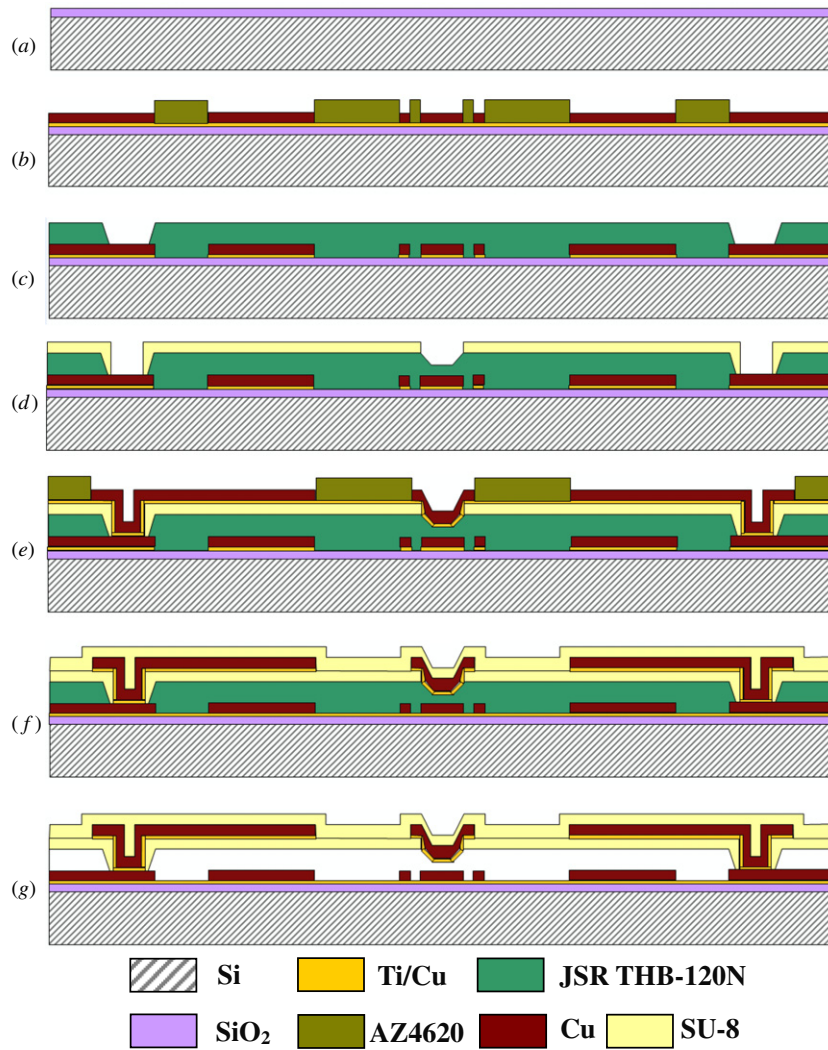


Figure 2. The schematic process flow of the proposed SU-8 serial MEMS switch.

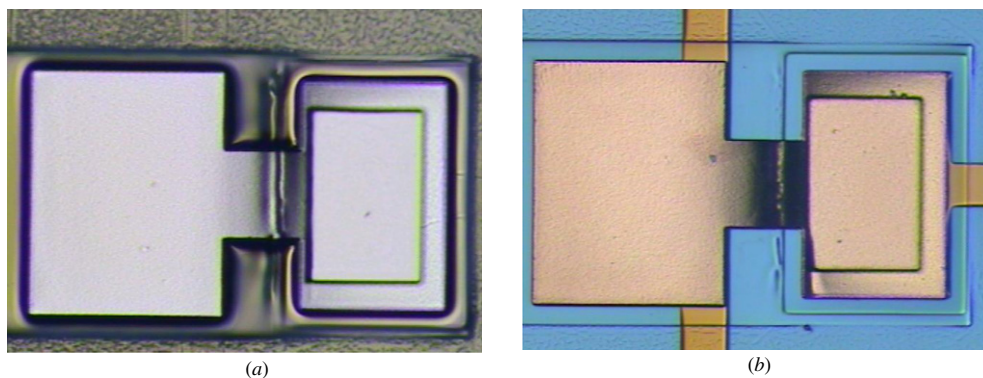


Figure 3. Optical micrographs of the enlarged view on the area of the driving electrode of the switch (a) before and (b) after sacrificial JSR layer removal.

under an optical microscope due to the transparency of SU-8 to visible light. It is noted that the average surface roughness of electroplated Cu characterized by an atomic force microscope (AFM), as shown in figure 4, has been well controlled by the aforementioned current density so as to get a good contact surface. The roughness of about 12.26 nm indicates that

our electroplating process is as good as the published results [11, 12].

3. Experimental results and discussions

The driving voltage of the as-fabricated SU-8 switch is determined from the measurement of dc contact resistance

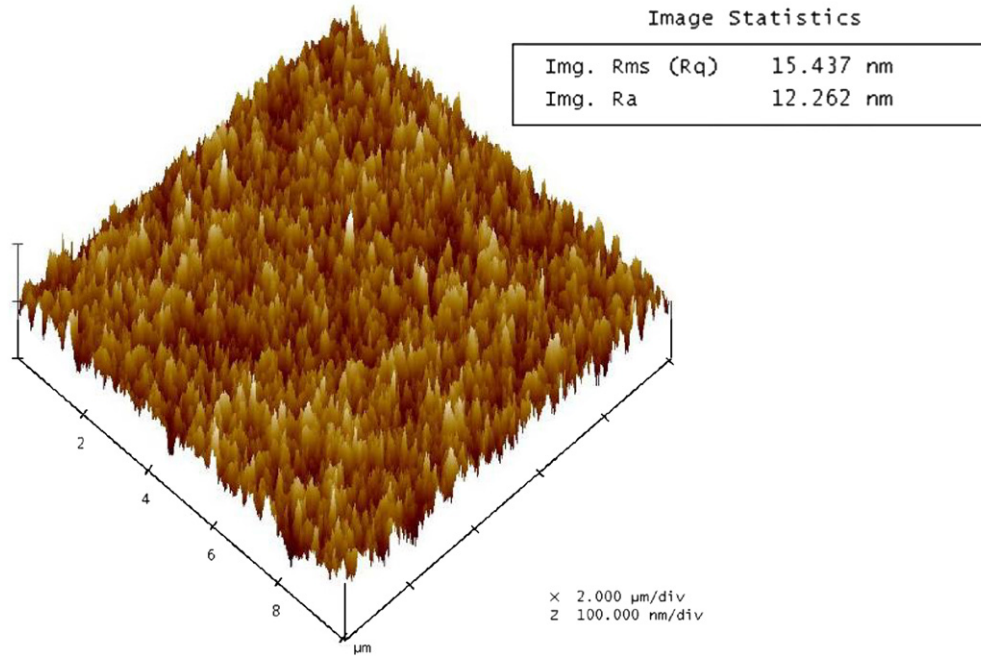


Figure 4. The AFM 3D profile image and average roughness of the electroplated Cu surface.

versus driving voltage. The contact resistance, R_C , is derived as follows:

$$R_C = \frac{R_{on} - R_{GND}}{2}, \quad (1)$$

where R_{on} and R_{GND} are the resistance of the signal line of the CPW at the ‘on’ state and the measured resistance of the ground line, respectively. The resistance measurement of the as-fabricated switch shows that the device with the input of 63 V will have an electrical contact with a contact resistance of 24.38 Ω. With the increase of the input voltage up to 92 V, the contact resistance will decrease to ~2.87 Ω which is close to the previously reported Cu–Cu contacts loaded with the contact force of ~20 μN [13].

Figure 5 shows the experimental setup for the as-fabricated switch RF measurement where Infinity I50-GSG-150 μm probes connected to an Agilent E8364B PNA network analyzer are utilized for the measurement of the S parameter and Cascade EP-03-150 W power bypass probes connected to serially linked Good Will Instrument PPT-1830 power supplies are utilized for actuating the switch. Figure 6 shows the measurement and simulation results of the SU-8 switch. The simulation results are calculated by an Ansoft high-frequency structure simulator (HFSS) with the conditions of 6 Ω cm silicon resistivity and 2 Ω contact resistance for each contact. Insertion loss and isolation represent the S_{21} performance of the switch operated at the ‘on’ and ‘off’ states, respectively. While the contact metal fully contacts with two disconnected CPW signal lines, i.e. at the ‘on’ state, the insertion loss is about -3.46 dB at 4 GHz/-4.48 dB at 12 GHz that includes the intrinsic loss of two disconnected CPW, contact loss and the loss originating from the contact metal in the switch. On the other hand, the isolation represents the performance of the switch operated at the ‘off’ state. Due to the large contact distance between the switch metal contact and the

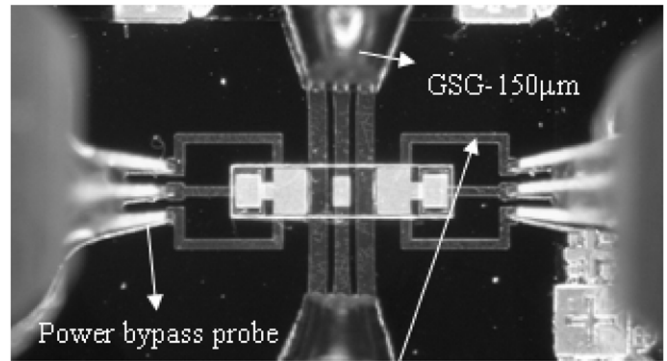


Figure 5. High-frequency measurement setup for the MEMS switch.

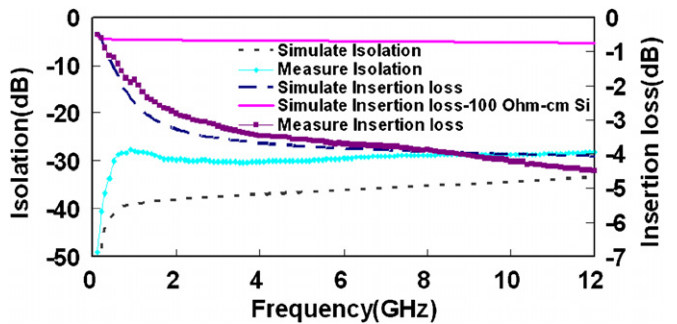


Figure 6. The measurement and simulation results of the SU-8 switch while the switch is operated at the ‘on’ and ‘off’ states.

CPW while the switch is operated at the ‘off’ state, the switch has a good isolation of -49.09 dB at 100 MHz/-28.23 dB at 12 GHz.

Although the switch performance of -4.48 dB insertion loss and -28.23 dB isolation at 12 GHz is worse than the

reported results [7, 14], the high insertion loss can be attributed to the substrate loss from the low resistivity of a Si substrate while the signal is transmitted along the 1000 μm long CPW. According to the simulation as shown in figure 6, the insertion loss can be greatly reduced down to -0.75 dB at 12 GHz once the resistivity of the Si substrate increases up to 100 $\Omega\text{ cm}$. Since the contact loss in the switch is around -0.38 dB without counting the CPW loss, which is comparable to the latest published Au contact switch whose loss is about -0.37 dB [14], it indicates that the as-fabricated switch performance can be further improved using the flexible organic substrate instead of the silicon substrate and a shorter transmission line to effectively reduce substrate, metal resistive losses. Nevertheless, the SU-8 process indeed provides an alternative approach for the fabrication of MEMS switches with a decent RF performance.

The bending moments M_e of a sandwich structure cantilever beam can be calculated as follows [15]:

$$M_e = \sigma_a w t_a (y_e - y_a) - \sigma_b w t_b (y_b - y_e) - \sigma_c w t_c (y_c - y_e) + \frac{1}{6} \nabla \sigma_b w t_b^2, \quad (2)$$

where t_a , t_b and t_c are the thicknesses of each layer; y_a , y_b and y_c are the neutral axes of each layer; σ_a , σ_b and σ_c are the mean stresses of each layer; and w , y_e and $\nabla \sigma_b$ are the width of the beam, the neutral axis of the sandwich beam and the stress gradient of the middle layer, respectively. If the top and bottom layers are made of identical material and have the same thickness, then y_e is equal to y_b . Therefore, the first three terms of equation (2) can be fully canceled to minimize the residual stress. However, it is inevitable to have process non-uniformity resulting in thickness difference of two SU-8 layers, which is 3 and 5 μm , respectively, at the laboratory and the residual stress cannot be eliminated in our case. Since we do not observe any deformation of the sandwich clamped-clamped beam by an optical microscope after sacrificial layer release, this means that the residual stress has been reduced and it would not dramatically induce an unwanted effect on the proposed sandwich beam. The details of residual stress characterization in each layer of the sandwich beam still need further investigation. In addition, the spin coating has been widely studied for film planarization [16, 17]. SU-8 is a spin-coated PR whose thickness can be well controlled in terms of the spraying amount of the PR, spinning speed and time, soft baking temperature and time for reflowing, and so on. In fact, the non-uniformity problem can be well resolved with further process optimization.

Figure 7 shows the preliminary cycling test results of the SU-8 switch which has been actuated at 92 V 2000 times. The result shows that the variance of contact resistances of Cu–Cu contacts is less than 10%. No drastic contact resistance increase has been found. Nevertheless, the long-term reliability issue needs more research work and the cycling test is still underway. Besides, the measured contact resistance is still larger than that of the Au contact [18]. Since the residual stress which may influence the contact resistance is reduced by the sandwich structure, the contact resistance could be mainly attributed to very thin native oxide formation on the Cu surface. For future applications of the switch to flexible electronics,

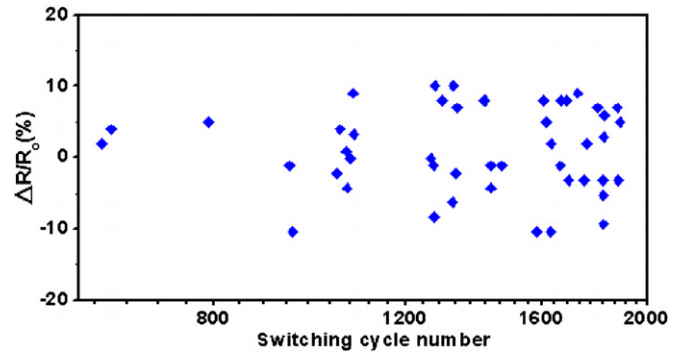


Figure 7. The percentage of contact resistance deviation of the SU-8 MEMS switch for the preliminary 2000 times cycling test.

the insertion loss of the switch can be further improved using the SU-8 low-temperature process combined with Au plating instead of Cu plating, and related process development is also underway.

4. Conclusions

A low-temperature micromachining process for the fabrication of SU-8 RF MEMS series switches has been developed and demonstrated. The RF performance of the switch includes better than -4.48 dB insertion loss and -28.23 dB signal isolation up to 12 GHz. Since the Cu–Cu contact resistance is about 2.87 Ω while the switch is actuated at 92 V, the high insertion loss mainly resulted from substrate loss. Simulation shows that the insertion loss can be further improved to -0.75 dB as long as the substrate resistivity is increased up to 100 $\Omega\text{ cm}$. Owing to the low processing temperature characteristics, which can be kept below 135 $^{\circ}\text{C}$, and the simple spin-coating process, the proposed micromachining process can provide an alternative for making other RF MEMS components such as tunable capacitor, inductor and antenna for flexible RF applications.

Acknowledgments

This work was supported by the National Science Council (Taiwan) under Grant NSC 99-2220-E-009-059 and in part by MOEA under Grant 99-EC-17-A-03-S1-005 Project. The authors would like to thank Gersterltec for their SU-8 material properties support and NCHC (National Center of High-Performance Computing) for the simulator support.

References

- [1] Chang H P, Qian J, Cetiner B A, Flaviis F D, Bachman M and Li G P 2005 Design and process considerations for fabricating RF MEMS switches on printed circuit boards *J. Microelectromech. Syst.* **14** 1311–22
- [2] Guo L H, Zhang Q X, Li H Y, Liao E B, Bera L K, Loh W Y, Kuo C C, Lo G Q, Balasubramanian N and Kwong D L 2005 Successful transferring of active transistors, RF-passive components and high density interconnect from bulk silicon to organic substrates *IEDM Tech. Dig.* pp 675–8

- [3] Yuan H-C and Ma Z 2006 Microwave thin-film transistors using Si nanomembranes on flexible polymer substrate *Appl. Phys. Lett.* **89** 212105–7
- [4] Kingsley N, Anagnostou D E, Tentzeris M M and Papapolymerou J 2007 RF MEMS sequentially reconfigurable Sierpinski antenna on a flexible organic substrate with novel DC-biasing technique *J. Microelectromech. Syst.* **16** 1185–92
- [5] Zhang Q X, Yu A B, Guo L H, Kumar R, Teoh K W, Liu A Q, Lo G Q and Kwong D L 2006 Development of RF MEMS switch on flexible organic substrate with wafer transfer technology (WTT) *IEEE Electronic Components and Technology Conf.* pp 523–7
- [6] Ramadoss R, Lee S, Lee Y C, Bright V M and Gupta K C 2006 RF-MEMS capacitive switches fabricated using printed circuit processing techniques *J. Microelectromech. Syst.* **15** 1595–604
- [7] Rebeiz G M 2003 *RF MEMS Theory, Design, and Technology* (Hoboken, NJ: Wiley)
- [8] Shi Y and Kim S G 2005 A lateral, self-cleaning, direct contact MEMS switch *IEEE Int. Conf. on MEMS* pp 195–8
- [9] Hyman D *et al* 1999 Surface-micromachined RF MEMS switches on GaAs substrates *Int. J. RF Microw. Comput.-Aided Eng.* **9** 348–61
- [10] JSR Corp. <http://www.jsrmicro.com>
- [11] Kang M S, Kim S K and Kim J J 2005 A novel process to control the surface roughness and resistivity of electroplated Cu using thiourea *Japan. J. Appl. Phys.* **44** 8107–9
- [12] Ooka M and Yokoyama S 2006 Effect of H₂ addition during Cu thin-film sputtering *Japan. J. Appl. Phys.* **45** 9058–62
- [13] Liu Q, McCormick D T, Roberts R C and Tien N C 2007 Nanoscale Al–Al and Cu–Cu contacts *14th Transducers Conf.* pp 1593–6
- [14] Cho I J, Song T, Baek S H and Yoon E 2005 A low-voltage and low-power RF MEMS series and shunt switches actuated by combination of electromagnetic and electrostatic forces *IEEE Trans. Microw. Theory Tech.* **53** 2450–7
- [15] Tsai C Y and Chen T L 2010 Design, fabrication and calibration of a novel MEMS logic gate *J. Micromech. Microeng.* **20** 095021
- [16] Chou F C, Wu P Y and Gong S C 1998 Analytical solutions of film planarization during spin coating *Japan. J. Appl. Phys.* **37** 4321–7
- [17] Peurrung L M and Graves D B 1993 Spin coating over topography *IEEE Trans. Semicond. Manuf.* **6** 72–6
- [18] Kwon H, Choi D J, Park H, Lee H C, Park Y H, Kim Y D, Nam H J, Joo Y C and Bu J U 2007 Contact materials and reliability for high power RF-MEMS switches *IEEE Int. Conf. on MEMS* pp 231–4